Article

Cell Reports

Serine 62-Phosphorylated MYC Associates with Nuclear Lamins and Its Regulation by CIP2A Is Essential for Regenerative Proliferation

Graphical Abstract

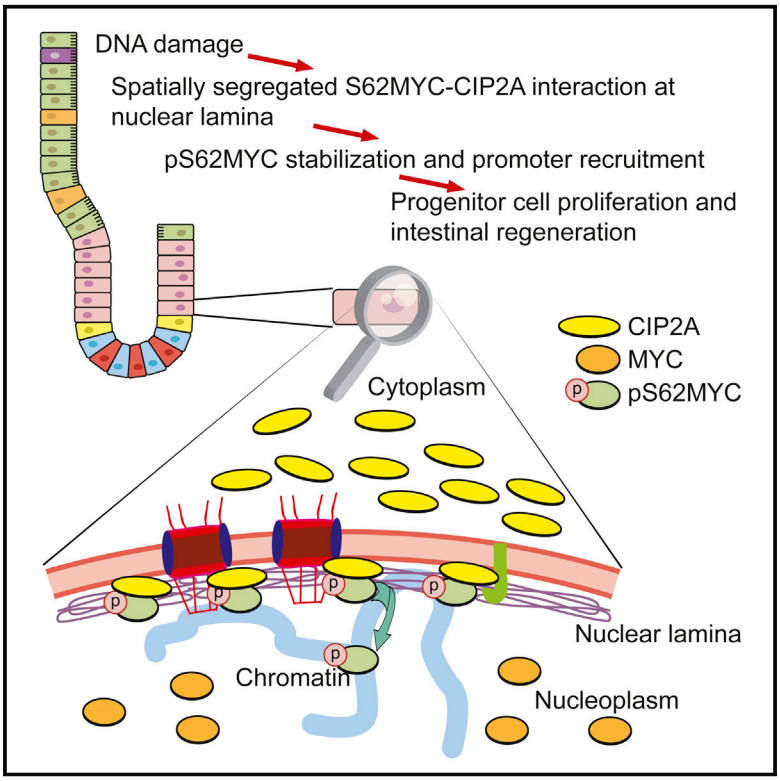

Highlights

- Serine 62-phosphorylated MYC is regulated by CIP2A in Lamin A/C-associated complexes
- CIP2A is required for MYC S62 phosphorylation during proliferation induction in vivo
- MYC activity can be systemically targeted without detrimental physiological effects
- We identify a phosphorylation switch defining the DNA damage response in vertebrates

Authors

Kevin Myant, Xi Qiao, Tuuli Halonen, ..., Rosalie C. Sears, Owen J. Sansom, Jukka Westermarck

Correspondence

o.sansom@beatson.gla.ac.uk (O.J.S.), jukwes@utu.fi (J.W.)

In Brief

Myant et al. demonstrate a specific essential phosphorylation event for in vivo activity of the oncoprotein MYC. This phosphorylation and MYC-mediated proliferation in vivo requires the PP2A phosphatase inhibitor protein CIP2A. Therefore, CIP2A targeting may allow the inhibition of MYC activity for therapies in hyperproliferative diseases.

Myant et al., 2015, Cell Reports *12*, 1019–1031
August 11, 2015
http://dx.doi.org/10.1016/j.celrep.2015.07.003

CellPress

Cell Reports
Article

Serine 62-Phosphorylated MYC Associates with Nuclear Lamins and Its Regulation by CIP2A Is Essential for Regenerative Proliferation

Kevin Myant,[1,6,8] Xi Qiao,[2,3,6] Tuuli Halonen,[2] Christophe Come,[2] Anni Laine,[2] Mahnaz Janghorban,[4] Johanna I. Partanen,[5] John Cassidy,[1] Erinn-Lee Ogg,[1] Patrizia Cammareri,[1] Tiina Laiterä,[2] Juha Okkeri,[2] Juha Klefström,[5] Rosalie C. Sears,[4] Owen J. Sansom,[1,7,*] and Jukka Westermarck[2,3,7,*]

[1]The Beatson Institute for Cancer Research, Glasgow G61 1BD, UK
[2]Turku Centre for Biotechnology, University of Turku and Åbo Akademi University, 20520 Turku, Finland
[3]Department of Pathology, University of Turku, 20520 Turku, Finland
[4]Department of Molecular and Medical Genetics and Knight Cancer Institute, Oregon Health and Science University, Portland, OR 97239, USA
[5]Research Programs Unit, Translational Cancer Biology and Institute of Biomedicine, University of Helsinki, 00014 Helsinki, Finland
[6]Co-first author
[7]Co-senior author
[8]Present address: Edinburgh Cancer Research Centre, IGMM, Edinburgh EH4 2XU, UK
*Correspondence: o.sansom@beatson.gla.ac.uk (O.J.S.), jukwes@utu.fi (J.W.)
http://dx.doi.org/10.1016/j.celrep.2015.07.003

SUMMARY

An understanding of the mechanisms determining MYC's transcriptional and proliferation-promoting activities in vivo could facilitate approaches for MYC targeting. However, post-translational mechanisms that control MYC function in vivo are poorly understood. Here, we demonstrate that MYC phosphorylation at serine 62 enhances MYC accumulation on Lamin A/C-associated nuclear structures and that the protein phosphatase 2A (PP2A) inhibitor protein CIP2A is required for this process. CIP2A is also critical for serum-induced MYC phosphorylation and for MYC-elicited proliferation induction in vitro. Complementary transgenic approaches and an intestinal regeneration model further demonstrated the in vivo importance of CIP2A and serine 62 phosphorylation for MYC activity upon DNA damage. However, targeting of CIP2A did not influence the normal function of intestinal crypt cells. These data underline the importance of nuclear organization in the regulation of MYC phosphorylation, leading to an in vivo demonstration of a strategy for inhibiting MYC activity without detrimental physiological effects.

INTRODUCTION

An understanding of the mechanisms controlling MYC function in vivo is critical for the development of MYC-targeted therapies. By using loss-of-function genetic models, MYC has been shown to be required for proliferation induction in several types of normal cells, including fibroblasts, intestinal progenitors, and lymphoid B and T cells (de Alboran et al., 2001; Mateyak et al., 1997; Sansom et al., 2007; Trumpp et al., 2001). Moreover, it has been demonstrated recently that MYC expression is essential for intestinal crypt regeneration in response to either irradiation-induced or chemically induced DNA damage (Ashton et al., 2010; Athineos and Sansom, 2010). Although these studies have convincingly demonstrated the critical role for a MYC dose for an in vivo proliferation response, they are not particularly informative regarding the endogenous mechanisms that regulate MYC's activity by post-translation modifications in vivo.

The induction of c-*myc* mRNA expression after proliferative stimuli is very rapid and transient, whereas the expression of the MYC protein is more sustained because of increased protein stability (Hann, 2006; Lutterbach and Hann, 1994; Sears et al., 1999; Thomas and Tansey, 2011). Cell culture and in vitro studies have revealed that the MYC protein is heavily regulated by various post-translational modifications (Hann, 2006; Lüscher and Vervoorts, 2012). Moreover, several different domains of MYC are implicated to be critical for its activity in regulating the expression of its numerous target genes as well as for proliferation regulation (Hann, 2006; Lüscher and Vervoorts, 2012; Meyer and Penn, 2008). Remarkably, despite this knowledge, it has not been established which of the numerous MYC post-translational modifications define(s) MYC's activity in vivo.

A cancerous inhibitor of PP2A, CIP2A, is a recently identified human oncoprotein (Junttila et al., 2007; Khanna et al., 2013). Consistent with its role as an inhibitor of ubiquitous serine/threonine phosphatase PP2A that regulates the activity of numerous cellular signaling pathways (Janssens and Goris, 2001), CIP2A has been shown to regulate the phosphorylation and activity of Akt, DapK, E2F1, MYC, and mTORC (Khanna et al., 2013; Puustinen et al., 2014). However, except for its role in promoting spermatogenesis (Ventelä et al., 2012), the physiological role of CIP2A is unclear. Also, in vivo, the only so far validated CIP2A target protein is E2F1 in a murine model of breast cancer (Laine et al., 2013).

Very recent studies have demonstrated a critical function for nuclear lamina-associated structures in gene regulation and chromosomal organization (Arib and Akhtar, 2011; Bukata et al., 2013; Dechat et al., 2010; Kind et al., 2013; Zullo et al., 2012). In this work, we demonstrate that serine 62 phosphorylation promotes MYC recruitment to nuclear Lamin A/C-associated structures (LASs), where its interaction with CIP2A is required for retaining this localization and MYC activity. Moreover, by using MYC loss-of-function and phosphorylation mutants and the attenuation of CIP2A, we provide a comprehensive in vivo approach to validate the importance of MYC serine 62 phosphorylation for the organismal proliferation response. Together, these results demonstrate an endogenous mechanism that defines the activation of MYC phosphorylation in vivo. Because CIP2A is dispensable for normal tissue function and mouse well-being, these results also indicate potential therapeutic opportunities for the inhibition of MYC activity in vivo without detrimental effects on normal physiology.

RESULTS

Characterization of the Spatial Nuclear Organization of the CIP2A-MYC Interaction

To provide a spatial understanding of the CIP2A-mediated regulation of MYC, we first analyzed the subcellular distribution of CIP2A in HeLa cells in which CIP2A constitutively promotes the expression of serine 62-phosphorylated MYC and MYC activity (Junttila et al., 2007; Niemelä et al., 2012). Consistent with immunofluorescence staining analyses (Figure 1A), the great majority of CIP2A was expressed in the cytoplasmic fraction of cells (Figure 1B), but a small fraction was expressed in the nucleus and especially in the insoluble nuclear fraction together with Lamin A/C (Figure 1B). Importantly, a proximity ligation assay (PLA) with CIP2A and Lamin A/C primary antibodies revealed a clear CIP2A-Lamin A/C association (Figure 1C). Interestingly, the CIP2A interaction with Lamin A/C is not restricted to nuclear lamina but is also observed in discrete intranuclear dots. This is fully consistent with an immunofluorescence (IF) analysis of the intranuclear localization of Lamin A/C (Figure 1C) and recently published data showing that many Lamin A/C-containing structures are mobile in the nuclei (Capelson et al., 2010; Kind et al., 2013).

Next we used a PLA to analyze whether MYC interacts with Lamin A/C. MYC-Lamin A/C association was observed with a pattern that resembled CIP2A-Lamin A/C association. The majority of signals were detected in the nuclear periphery, but very clear intranuclear interactions were also observed (Figure 1D; Figure S1A). Importantly, the CIP2A-MYC association, as shown by PLA, also co-localized with Lamin A/C at the nuclear lamina, although, again, intranuclear interactions were also observed (Figure 1E, b and insets). Serine 62 phosphorylation of MYC is important for MYC-mediated gene regulation and protein stability (Hann, 2006; Lüscher and Vervoorts, 2012). Notably, PLA with pS62MYC antibody and CIP2A revealed a similar pattern of interaction at the nuclear lamina as with an antibody that detects the total MYC pool (Figures 1E, c and d, and 1F), indicating that the form of MYC that interacts with CIP2A is phosphorylated on serine 62. To see whether the pattern of CIP2A-pS62MYC PLA signals, both at the nuclear lamina and in the nuclear interior, corresponds to the distribution of pS62MYC protein, the cells were examined by pS62MYC immunofluorescence staining. As shown in Figure 1G, the distribution of pS62MYC did resemble the nuclear lamina-enriched punctuate pattern seen with CIP2A-pS62MYC PLA, although, based on fewer CIP2A-pS62MYC PLA signals (Figure 1E) compared with signals observed with immunofluorescence staining (Figure 1G), it is apparent that only a certain fraction of pS62MYC interacts with CIP2A at any given moment. Importantly, the distribution pattern of total MYC did not show a similar punctuate pattern as that observed with pS62MYC IF or by CIP2A-MYC PLA, and there was no particular enrichment of total MYC IF signals at the nuclear periphery (Figure 1G). This further indicates that the form of MYC with which CIP2A interacts at the LAS is pS62MYC.

These results reveal a selective spatial distribution of pS62MYC in complex with CIP2A at the LAS.

The Major Fraction of pS62MYC Is Bound to Proteinaceous Nuclear Structures via a DNA-Independent Mechanism

Next we addressed, with a classical salt fractionation protocol, the biochemical basis of the CIP2A and pS62MYC association with the LAS. As expected, we found that increasing the NaCl concentration released both pS62MYC and MYC from the insoluble to the soluble nuclear fraction (Figure 1H; Figure S1B). However, compared with MYC, a significant fraction of CIP2A remained insoluble even in the presence of 500 mM NaCl, and, as expected, H3 was entirely resistant to this treatment (Figure 1H; Figure S1B). To further study the potential role of DNA binding in the nuclear segregation of CIP2A and pS62MYC to the LAS, the insoluble nuclear fractions isolated without detergent treatment were subjected to DNAase (benzonase) treatment, and the expression of pS62MYC, total MYC, MAX, and CIP2A was compared between the insoluble pellet and the benzonase eluate. To verify the efficacy of elution of DNA-bound proteins by benzonase, we show that approximately 70% of the total H3 was eluted by this treatment (Figures 1I and 1J). Surprisingly, only approximately 20% of pS62MYC, total MYC, or MAX was eluted by benzonase treatment (Figures 1I and 1J), whereas, in comparison with H3 and MYC, negligible amounts of CIP2A were detected in benzonase-treated eluates (Figures 1I and 1J).

These results indicate that CIP2A and the majority of pS62MYC are bound to the proteinaceous component of the LAS. Moreover, the association of pS62MYC with the LAS seems to be mediated by an ionic interaction.

Serine 62 Phosphorylation of MYC Drives Its Association with the LAS, and CIP2A Is Required to Retain This Localization

Based on the results above, we rationalized that serine 62 phosphorylation of MYC may promote the recruitment of MYC to the LAS and that, rather than chromatin binding, its interaction with CIP2A may be required to retain pS62MYC in these sites of chromatin re-organization and transcription regulation (Arib and Akhtar, 2011; Kind et al., 2013; Zullo et al., 2012). To study this, we

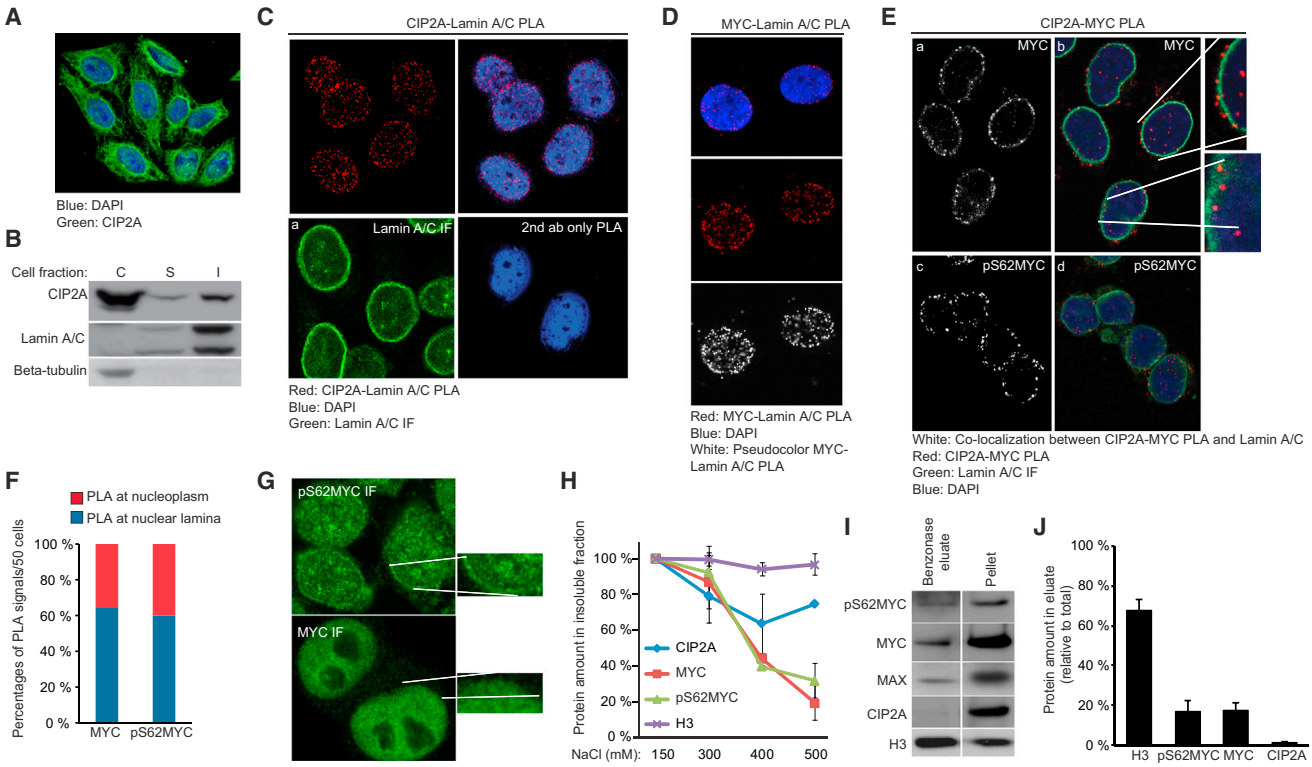

Figure 1. CIP2A and Serine 62-Phosphorylated MYC Interact at Lamin A/C-Associated Proteinaceous Nuclear Structures

(A) Immunofluorescent staining of CIP2A in HeLa cells.

(B) Analysis of subcellular distribution of CIP2A in cytoplasmic (C) soluble nuclear (S) and insoluble nuclear (I) fractions of HeLa cells by high-salt (400 mM NaCl) nuclear extraction. Lamin A/C and β-tubulin represent nuclear and cytoplasmic markers, respectively.

(C) PLA analysis of the CIP2A-Lamin A/C association in HeLa cells. The specificity of PLA is shown by the lack of PLA signals in a secondary antibody-only control panel. a: immunofluorescence analysis of Lamin A/C distribution both in the nuclear lamina as well as in the nucleoplasm. ab, antibody.

(D) PLA analysis of the MYC-Lamin A/C association in HeLa cells. White dots are pseudocolor MYC-Lamin A/C PLA signals.

(E) PLA analysis of the CIP2A-MYC and CIP2A-pS62MYC association in HeLa cells. a–d: co-localization of CIP2A-MYC and CIP2A-pS62MYC PLA signals with Lamin A/C (white dots). The insets in b show detailed images of the association of the CIP2A-MYC PLA signal with Lamin A/C.

(F) Quantitation of CIP2A-MYC and CIP2A-pS62MYC PLA signals at the nuclear lamina and nucleoplasm from (E, b and d).

(G) Immunofluorescence analysis of pS62MYC and total MYC nuclear distribution. The insets highlight the difference in staining pattern between pS62MYC and MYC.

(H) Quantification of the relative expression of the indicated proteins in the insoluble fraction of HeLa cells subjected to salt extraction fractionation with increasing NaCl concentrations.

(I) Analysis of the DNA dependence of the CIP2A, pS62MYC, and MYC association with the insoluble nuclear fraction. Histone H3 was used as a control for the efficacy of elution of DNA-bound proteins.

(J) Quantitation of the protein amount in benzonase eluate relative to the total amount from (I). The samples were loaded on the same gel. Error bars represent SEM (n = 3).

examined the distribution of exogenously expressed wild-type MYC and two mutants, S62A and T58A MYC, between the insoluble and soluble nuclear fractions. We have shown previously that the functionally inactive MYC S62A mutant (Benassi et al., 2006; Sears et al., 2000) does not interact with CIP2A in human cells (Junttila et al., 2007), whereas the MYC T58A mutant, which is a functional mimic of serine 62-phosphorylated MYC (Benassi et al., 2006; Hann, 2006; Wang et al., 2011; Yeh et al., 2004), retains full CIP2A-interacting capacity (Junttila et al., 2007). Notably, the S62A mutant of MYC showed a clearly reduced accumulation to the insoluble nuclear fraction compared with wild-type MYC, whereas the CIP2A binding-competent T58AMYC accumulated very efficiently in the insoluble fraction (Figures 2A and 2B). These results are in agreement with PLA results demonstrating that the form of MYC that is associated with the LAS is pS62MYC (Figures 1E–1G). To further confirm that the distribution to the insoluble fraction reflects the differential association of MYC phosphorylation mutants with the LAS, we performed a PLA with V5 and Lamin A/C antibodies in cells expressing equivalent amounts of V5-S62AMYC or V5-T58AMYC (Figure S2). Consistent with other results, T58AMYC showed a clearly increased association with Lamin A/C compared with S62AMYC (Figure 2C).

The results above, together with a PLA and IF analysis of pS62MYC (Figures 1E and 1G), clearly demonstrate that serine 62 phosphorylation increases MYC's association with the LAS.

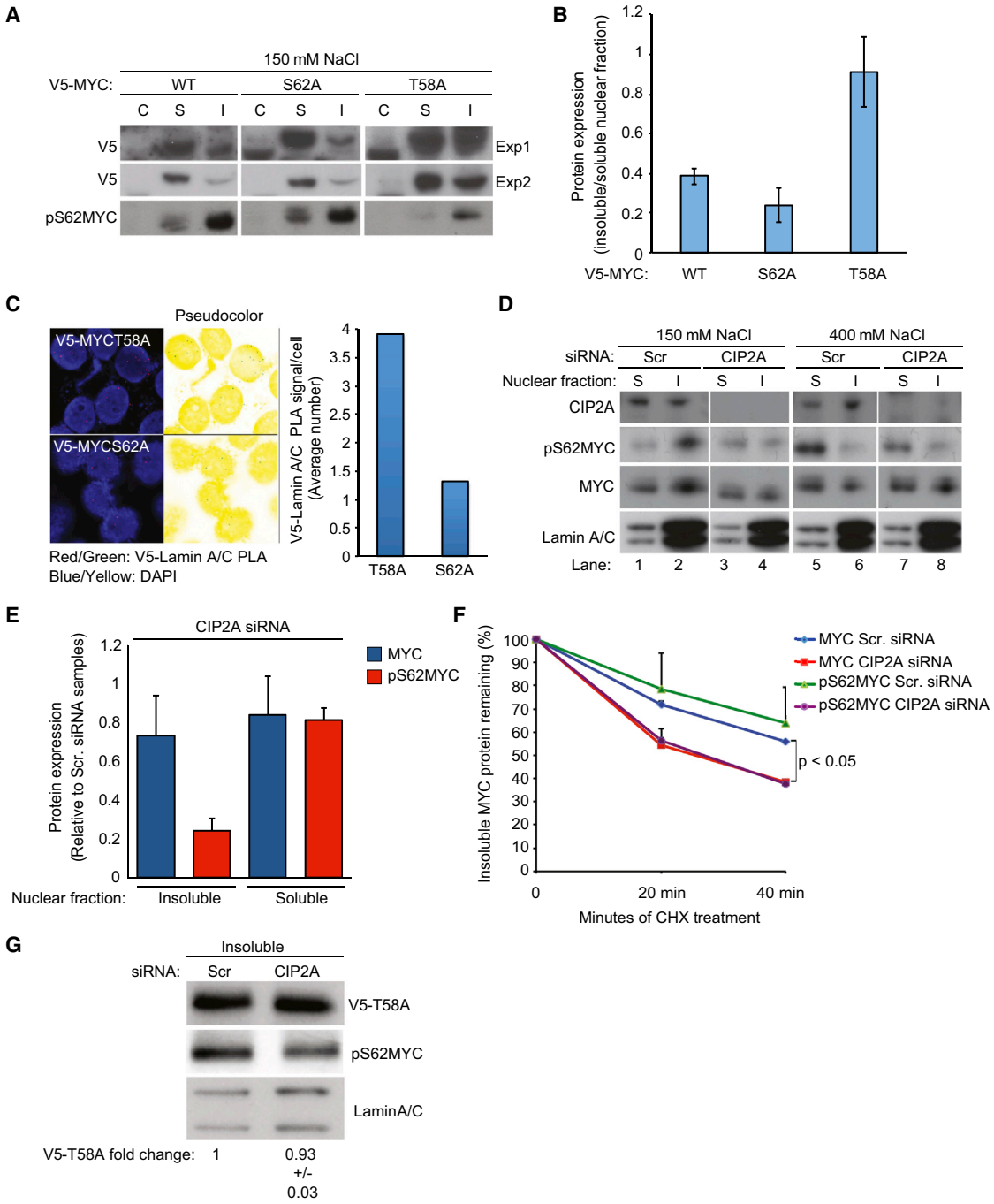

Figure 2. Serine 62 Phosphorylation of MYC Enhances Its Recruitment to Lamin A/C-Associated Nuclear Structures, and CIP2A Is Required to Retain This Localization

(A) Western blot analysis of the subnuclear distribution of exogenous V5-tagged WT, S62A, and T58A MYC and pS62MYC in HeLa cells. The fractionation was done with 150 mM NaCl. V5 antibody was used to detect WT MYC and the S62A and T58A MYC mutants. Exp, experiment.

(B) Quantitation of the ratio of V5-MYC between the insoluble and soluble nuclear fractions from (A). Shown is the mean ± SEM of two experiments.

(C) PLA analysis of the V5-Lamin A/C association in HeLa cells transfected with equivalent amounts of V5-MYCT58A or V5-MYCS62A mutant. Shown is a quantification of the average number of V5-Lamin A/C PLA signals per cell from 50 cells.

(D) Analysis of subnuclear portioning of pS62MYC and total MYC in CIP2A siRNA-transfected HeLa cells. The indicated salt extraction conditions were used to either retain MYC in (150 mM) or dissociate MYC from (400 mM) the insoluble fraction. Scr, scrambled.

(E) CIP2A depletion selectively affects pS62MYC localized to the insoluble fraction. Lanes 5 and 7 represent proteins that were extracted from the insoluble fraction, and the values for the effect of CIP2A depletion on pS62MYC and MYC expression in the insoluble fraction represent a comparison of lanes 2 and 5 for

(legend continued on next page)

However, whether CIP2A is relevant for the accumulation of MYC to the LAS has not yet been addressed. To this end, we studied the subnuclear distribution of pS62MYC and total MYC in CIP2A small interfering RNA (siRNA)-transfected cells. For the first part of this experiment, the nuclear proteins were extracted with low-salt buffer (150 mM NaCl) to preserve MYC's association with Lamin A/C. In support of our hypothesis, depletion of CIP2A inhibited the expression of pS62MYC in the Lamin A/C-enriched insoluble fraction, whereas the expression of total MYC was inhibited to a much smaller extent (Figures 2D, compare lanes 2 and 4, and 2E, insoluble). Importantly, the soluble fraction of pS62MYC was insensitive to CIP2A inhibition (Figures 2D, lanes 1 and 3, and 2E, soluble). To confirm that the CIP2A-sensitive pS62MYC pool corresponds to the salt-sensitive pool of MYC described in Figure 1H, insoluble proteins were extracted from CIP2A siRNA-transfected cells in the presence of 400 mM salt. Also, in this case, the CIP2A-sensitive pool of MYC was the pS62MYC eluted from the insoluble fraction (Figures 2D, lanes 5 and 7, and 2E).

CIP2A has been shown to prevent the degradation of MYC, and this effect is seen more profoundly with pS62MYC than with total MYC antibody (Junttila et al., 2007). Therefore, we examined whether CIP2A influences pS62MYC stability in the insoluble nuclear fraction. Indeed, a cycloheximide (CHX) chase experiment using both pS62MYC and MYC antibodies revealed a clear decrease in protein stability upon CIP2A RNAi in the insoluble nuclear fraction (Figure 2F). To confirm these results, we studied the impact of CIP2A depletion in the insoluble nuclear fraction on a T58A mutant that is resistant to PP2A-mediated destabilization (Yeh et al., 2004). Indeed, although CIP2A siRNA effects were observed by using the pS62MYC antibody, which detects both endogenous MYC and T58A, CIP2A depletion did not alter the accumulation of MYCT58A in the insoluble nuclear fraction (Figure 2G).

Together, the results so far demonstrate a function of serine 62 phosphorylation of MYC in promoting its association with the LAS. These results also demonstrate that CIP2A is not a universal regulator of MYC but that it selectively supports the stability of the LAS-associated pool of pS62MYC. As will be explained later, this newly characterized selectivity of CIP2A toward spatially segregated pS62MYC may explain the lack of detrimental physiological effects of systemic CIP2A inhibition (Laine et al., 2013; Ventelä et al., 2012) compared with the direct inhibition of MYC (Dubois et al., 2008; Soucek et al., 2008).

CIP2A Is Critical for Serum-Induced pS62MYC Expression and MYC-Mediated Proliferation Induction

Next we studied the relevance of CIP2A for mitogen-induced MYC regulation in mouse embryonic fibroblasts (MEFs) isolated from CIP2A-deficient ($CIP2A^{HOZ}$) mice (Laine et al., 2013; Ventelä et al., 2012) and their wild-type counterparts. Importantly, the loss of CIP2A clearly inhibited the serum-induced expression of serine 62-phosphorylated MYC (Figures 3A and 3B). Because immunoblotting of the same membrane with an antibody against total MYC showed an equal impairment in MYC accumulation (Figures 3A and 3B), we postulate that pS62MYC is the form of MYC that is most sensitive to mitogenic stimuli. This conclusion is supported by the preferential induction of pS62MYC protein expression, compared with total MYC, in wild-type MEFs treated with increasing concentrations of serum (Figures 3C and 3D). Importantly, c-*myc* mRNA induction was not impaired in serum-induced $CIP2A^{HOZ}$ MEFs (Figure 3E), further indicating that the effects on MYC are due to a CIP2A-dependent post-translational mechanism. Moreover, $CIP2A^{HOZ}$ MEFs showed a statistically significant decrease in bromodeoxyuridine (BrdU) incorporation (Figure 3F) and in the re-initiation of the cell cycle in response to serum induction (Figure 3G), consistent with results reported previously (Kim et al., 2013). Notably, the effects of CIP2A loss on MEF cell cycle regulation and proliferation are not as robust as those reported for MYC-null MEFs (de Alboran et al., 2001; Meyer and Penn, 2008; Perna et al., 2012), which is consistent with our conclusion that CIP2A loss affects only a sub-population of MYC. To provide additional and more direct evidence that CIP2A supports MYC's ability to drive cell cycle activity, we employed conditional MYC-estrogen receptor (ER)-expressing MCF-10A cells. In these cells, the addition of 4-hydroxytamoxifen activates MYC-ER, and this activation is sufficient to induce cell cycle re-entry in growth factor-deprived cultures (Nieminen et al., 2007). Notably, the inhibition of CIP2A expression resulted in loss of the ability of tamoxifen-activated MYC-ER to promote the cell cycle (Figure 3H). Importantly, CIP2A depletion did not affect MYC-ER fusion protein expression, confirming that CIP2A promotes MYC activity in proliferation induction (Figure 3I). Unlike in cancer cells (Laine et al., 2013), CIP2A inhibition in either MCF-10A or MEF cells did not affect E2F1 expression (Figure S3), providing further support for a selective role of CIP2A in regulating MYC activity in these cells.

Together, these results identify CIP2A as a critical endogenous regulator of MYC serine 62 phosphorylation and function during proliferation induction.

MYC Interacts with CIP2A in Mouse Intestinal Tissue

Intestinal regeneration after DNA damage induced by irradiation or by cisplatin treatment is fully dependent on MYC dose, and, therefore, it can be used as a model to address the MYC dependence of the in vivo proliferation response (Ashton et al., 2010; Athineos and Sansom, 2010; Finch et al., 2009; Muncan et al., 2006; Sansom et al., 2007). Similar to MYC, we observed CIP2A immunopositivity in cells of the intestinal crypt, with reduced expression in the differentiated cells of the villi (Figure 4A). The specificity of this staining pattern was demonstrated

scrambled siRNA and lanes 4 and 7 for CIP2A siRNA. The expression of MYC and pS62MYC in the soluble fraction was quantified between lanes 1 and 3. Shown is the mean + SEM of two experiments.

(F) Effect of CIP2A siRNA on endogenous pS62MYC stability in the insoluble nuclear fraction. The symbols denote the average pS62MYC and MYC expression levels at the indicated time points compared with non-CHX-treated cells. Shown is the mean ± SEM from three independent experiments.

(G) Western blot analysis of the expression of V5-tagged MYCT58A in the insoluble fraction in either scrambled or CIP2A siRNA-transfected HeLa cells. Endogenous pS62MYC is shown as a control for the functional perturbation of CIP2A function, and Lamin A/C was used as a loading control.

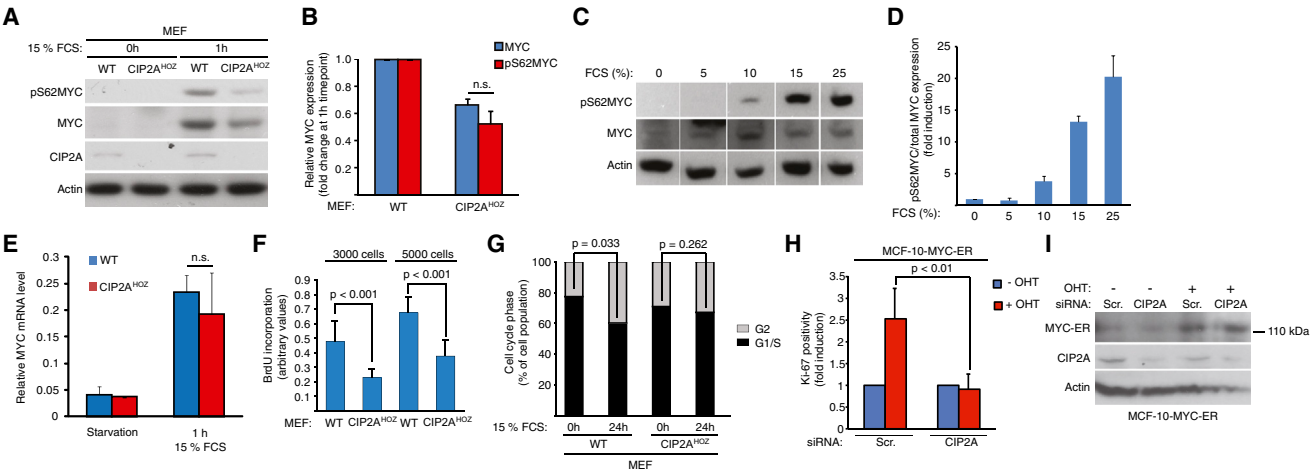

Figure 3. CIP2A Is a Critical Endogenous Regulator of MYC Phosphorylation and Function during Proliferation Induction

(A) Western blot analysis of pS62MYC, MYC, and CIP2A expression in serum-starved (0h) and serum-stimulated (1h) WT and *CIP2A*^{HOZ} MEFs. Shown is a representative result of four independent experiments with similar results.

(B) Quantitation of MYC and pS62MYC protein levels in response to serum induction and normalized to β-actin. Shown is the mean ± SEM of four experiments. n.s., not significant, Student's t test.

(C and D) Analysis of induction of pS62MYC protein expression compared with total MYC in wild-type MEFs treated with increasing concentrations of serum. Shown is the mean ± SEM of three experiments.

(E) RT-PCR analysis of MYC mRNA expression in serum-starved (0h) and serum-stimulated (1h) WT and *CIP2A*^{HOZ} MEFs. Shown is the mean ± SD of two independent experiments (Student's t test).

(F) BrdU incorporation of WT and *CIP2A*^{HOZ} MEFs 48 hr after seeding either 3,000 or 5,000 cells/well. Shown is the mean ± SD of three independent experiments (Student's t test).

(G) Cell cycle analysis of serum-starved (0h) and-serum stimulated (24h) WT and *CIP2A*^{HOZ} MEFs. Shown is the percentage of cells in either G1/S or G2 phase. Shown are mean values from three independent experiments (Student's t test).

(H) Induction of proliferation in MCF-10A-MYC-ER cells transfected with CIP2A or control siRNA (Scr) in hydroxytamoxifen (OHT)-treated cells (MYC active) and/or control cells (−OHT). Shown is the mean ± SD of induction of Ki-67-positive cells from three independent experiments (Student's t test).

(I) Western blot analysis of MYC-ER fusion protein (molecular weight, 110 kDa) expression in MCF-10A-MYC-ER cells transfected with CIP2A or control siRNA.

by a lack of specific staining in CIP2A^{HOZ} tissue (Figure 5A). Moreover, in situ PLA activity as an indication of an association between CIP2A and MYC proteins was detected in the nuclei of intestinal crypt cells (Figures 4B, a, 4C, and 4D). In contrast, a PLA using only secondary antibodies did not produce any detectable PLA activity (Figures 4B, b, and 4C). As an additional control, we show that, in comparison to wild-type tissue, a clearly smaller number of PLA-positive spots were observed in intestinal sections of CIP2A^{HOZ} mice (Figures 4E and 4F).

CIP2A Is Dispensable for Normal Intestinal Crypt Homeostasis but Promotes Intestinal Regeneration in Response to DNA Damage

MYC is essential for normal crypt structure in the adult intestine (Muncan et al., 2006; Soucek et al., 2008). On the other hand, recent analyses have demonstrated normal growth, weight, development, and lifespan of CIP2A^{HOZ} mice despite a lack of CIP2A expression in all studied organs (Laine et al., 2013; Ventelä et al., 2012). This suggests that the protein interaction between CIP2A and MYC in intestinal cells may not be essential for intestinal crypt homeostasis. In line with this hypothesis, a comparison of BrdU positivity and the number of paneth and goblet cells in the intestines of wild-type (WT) and CIP2A^{HOZ} mice did not reveal any indications of disturbance in proliferation or differentiation of intestinal crypts (Figure S4). Also, CIP2A^{HOZ} mice did not reveal any gross changes in crypt architecture compared with WT mice (Figure S4). These results demonstrate that CIP2A is dispensable for normal crypt function.

Notably, similar to MYC induction in response to DNA damage (Ashton et al., 2010; Athineos and Sansom, 2010), the regenerating intestinal tissue displayed a marked CIP2A upregulation both at the protein and mRNA levels, whereas the CIP2A^{HOZ} intestine remained CIP2A-deficient even under these conditions (Figures 5A and 5B). To determine whether increased CIP2A expression functionally contributes to MYC-dependent intestinal regeneration, crypt regeneration following irradiation was studied in CIP2A^{HOZ} mice and their wild-type controls. Control intestines demonstrated a robust regenerative response, and this response was significantly attenuated in the absence of CIP2A (Figures 5C and 5D). Additionally, the regenerating crypts observed in CIP2A^{HOZ} mice were significantly less proliferative than those of control mice (Figures 5E and 5F), whereas CIP2A loss did not acutely increase apoptosis induction in intestinal crypts after irradiation (Figure 5G). To verify that the CIP2A dependence of intestinal regeneration is a general phenomenon related to DNA damage, mice were treated systemically with the chemotherapy agent cisplatin. Importantly, in response to cisplatin treatment, CIP2A^{HOZ} intestines showed an even more dramatic perturbation in the regenerative and proliferative response than in response to irradiation (Figures 5H–5J).

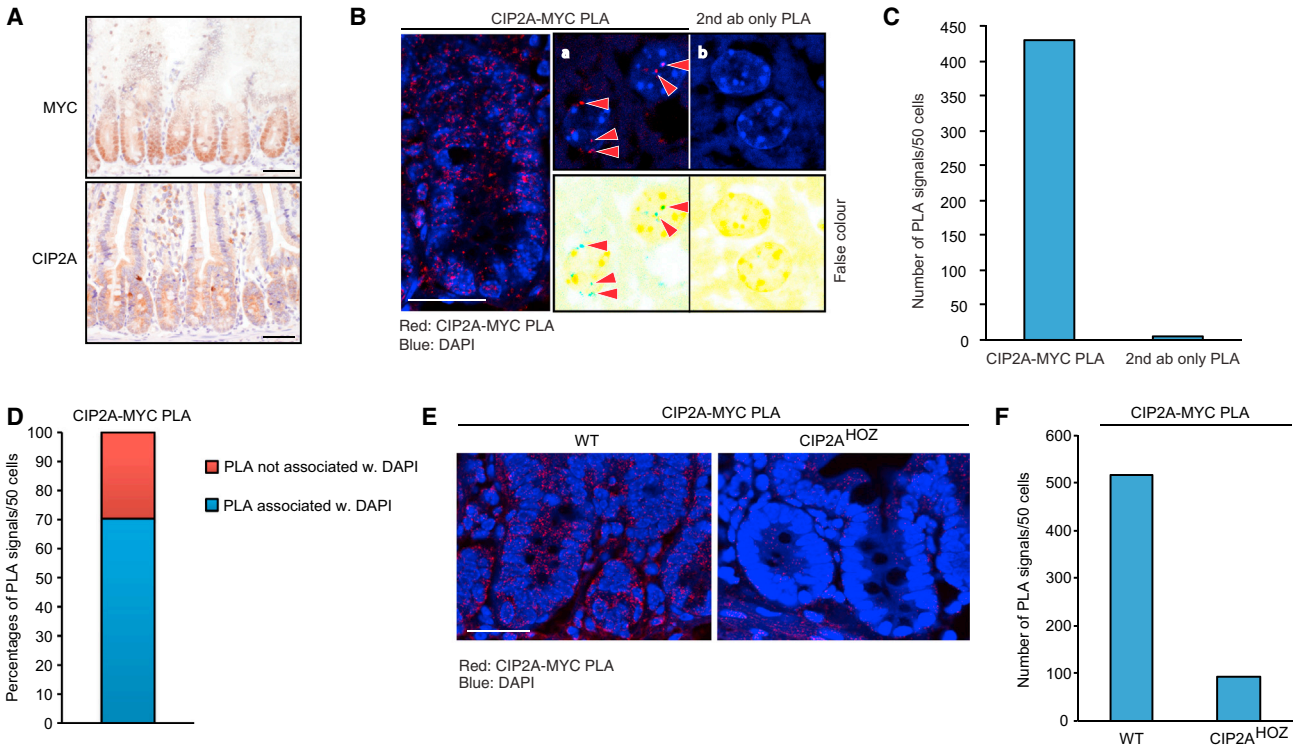

Figure 4. CIP2A Interacts with MYC in Intestinal Tissue

(A) Immunohistochemical staining of endogenous MYC (top) and CIP2A (bottom) expression in intestinal tissue. Scale bars, 50 μm.

(B) CIP2A and MYC physically associate in intestinal cells. Left: Red dots indicate the association of CIP2A and MYC proteins in intestinal tissue, as analyzed by PLA. Scale bar, 25 μm. a: red arrowheads indicate positive PLA signals in intestinal cell nuclei. b: no PLA signals were detected by using secondary antibodies (2nd ab) only.

(C) Quantitation of the number of PLA signals in 50 intestinal cells analyzed in (B).

(D) Quantitation of PLA signals that were associated with nuclear DAPI staining in (B).

(E) PLA analysis of the CIP2A-MYC association in WT and CIP2A^{HOZ} mouse intestinal tissues. Scale bar, 25 μm.

(F) Quantitation of number of PLA signals in 50 intestinal cells analyzed in (E).

To study whether CIP2A is expressed in Lgr5+ intestinal crypt stem cell-like cells, we exploited a transgenic mouse model expressing GFP under the Lgr5 promoter (Metcalfe et al., 2014). As shown in Figure 5K, CIP2A mRNA was relatively more expressed in the GFP-positive (Lgr5+) cell population than in Lgr5− cells. However, compared with OLFM4, which is a bona fide intestinal crypt stem cell factor (van der Flier et al., 2009), CIP2A was not enriched to the same extent (Figure 6K), which is also in accordance with positive CIP2A IHC staining in other intestinal crypt cells (Figure 4A).

These results demonstrate that CIP2A promotes MYC-dependent intestinal regeneration induced by DNA damage.

CIP2A Is Critical for the Transcriptional Activation of MYC Targets during Intestinal Regeneration

Next we asked whether the phenotypic outcome in intestinal tissue regeneration in CIP2A^{HOZ} mice is truly linked to the modification of MYC function. First, we investigated MYC expression levels in untreated intestines from control and CIP2A^{HOZ} mice and found no obvious difference (Figure 6A). In addition, upon regeneration, quantification of the intensity of MYC staining per cell within the crypt boundaries (Figure 6B, dashed line and insets) in 50 consecutive crypts/mouse revealed that MYC immunopositivity in *CIP2A*^{HOZ} mice within the crypt was at the same level as in WT crypts (Figure 6C). In addition, and similar to MEFs, c-*myc* mRNA was expressed at equal levels in regenerating WT and *CIP2A*^{HOZ} crypts (Figure 6D). However, fully consistent with our in vitro results showing that CIP2A selectively regulates pS62MYC (Figures 2D and 2E), the irradiation-induced expression of pS62MYC was inhibited in *CIP2A*^{HOZ} crypts (Figures 6E and 6F), and this correlated with the induction of proliferation assessed by Ki67 co-staining (Figures 6E and 6F).

Next we next performed a qRT-PCR analysis of irradiated wild-type and CIP2A^{HOZ} intestines on a number of MYC target genes involved in intestinal regeneration (Athineos and Sansom, 2010; Sansom et al., 2007). Of the genes analyzed, all were significantly downregulated in regenerating guts from *CIP2A*^{HOZ} mice compared with controls (Figure 6G). We also confirmed impaired MYC recruitment to the *tiam1* promoter upon CIP2A inhibition by siRNA in cultured cells (Figure S5). The MYC and CIP2A dependence of protein expression for selected MYC target genes was further confirmed using immunohistochemistry (IHC) (Figure 6H). Quantification of CDK4 and TIAM1 expression from sections adjacent sections to those from which MYC

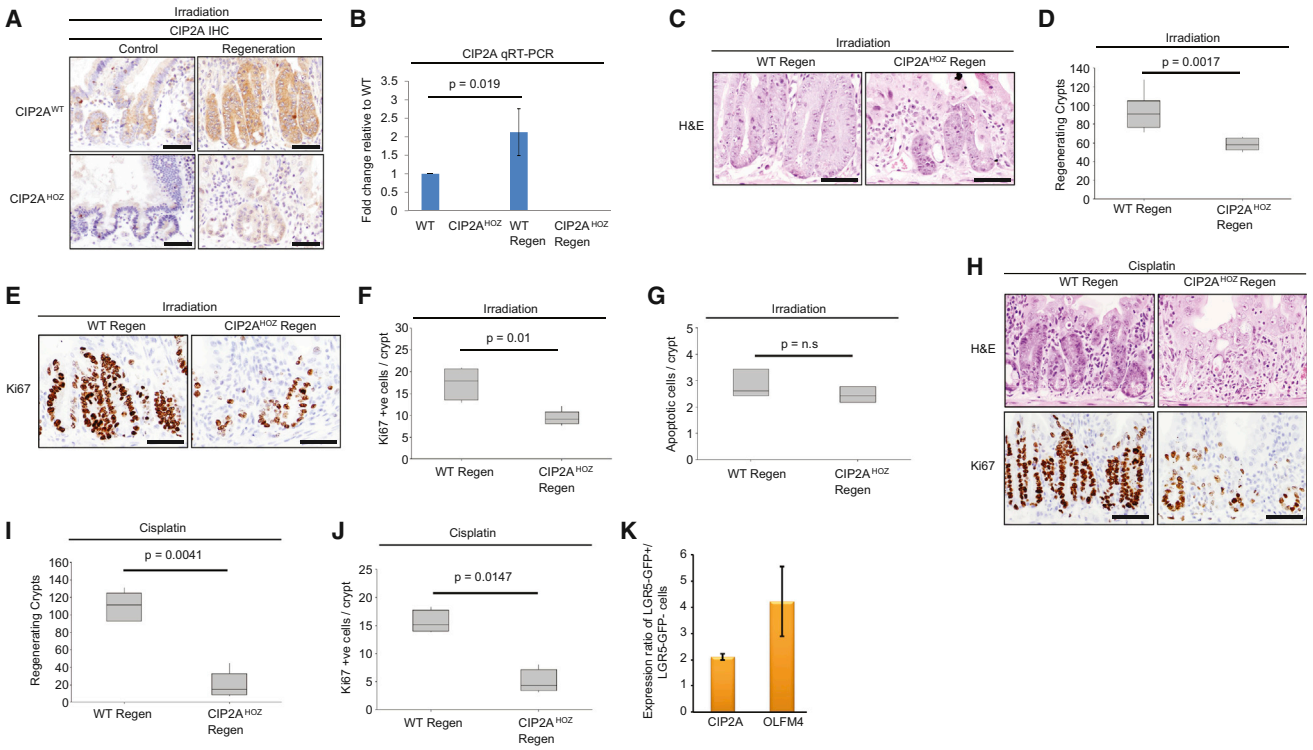

Figure 5. CIP2A Promotes Intestinal Regeneration in Response to DNA Damage

(A) Immunohistochemical staining of CIP2A in control and regenerating small intestines. Tissue from CIP2A-deficient (*CIP2A*^{HOZ}) mice was used to control for antibody specificity (bottom). Scale bars, 50 μm.

(B) qRT-PCR analysis for CIP2A in WT, *CIP2A*^{HOZ}, WT regenerating (Regen) and *CIP2A*^{HOZ} regenerating small intestine (Student's t test, n = 3). Error bars represent the mean ± SD.

(C) H&E staining of regenerating crypts from WT and *CIP2A*^{HOZ} intestines following irradiation. Scale bars, 50 μm.

(D) Scoring of a number of regenerating crypts in WT and *CIP2A*^{HOZ} intestines following irradiation (Mann-Whitney test, n = 7 versus 6).

(E) Ki67 staining of regenerating crypts from WT and *CIP2A*^{HOZ} intestines following irradiation. Scale bars, 50 μm.

(F) Scoring of number of Ki67-positive cells per crypt in WT and *CIP2A*^{HOZ} intestines following irradiation (Mann-Whitney test, n = 4 versus 5).

(G) CIP2A loss does not affect the intestinal apoptotic response following DNA damage. Shown is the scoring of a number of apoptotic cells per crypt in WT and *CIP2A*^{HOZ} intestines 6 hr post irradiation.

(H) H&E and Ki67 staining of regenerating crypts from WT and *CIP2A*^{HOZ} intestines following cisplatin treatment. Scale bars, 50 μm.

(I) Scoring of a number of regenerating crypts in WT and *CIP2A*^{HOZ} intestines following cisplatin treatment (Mann-Whitney, n = 6 versus 5).

(J) Scoring of a number of Ki67-positive cells per crypt in WT and *CIP2A*^{HOZ} intestines following cisplatin treatment (Mann-Whitney test, n = 4).

(K) Expression ratio of CIP2A and OLFM4 mRNA in GFP-LGR5-positive/LGR5 negative intestinal crypt cells after GFP-positive cell sorting. Error bars represent the mean ± SD.

expression was quantified (Figure 6B) confirmed the significant inhibition of expression of both of these MYC targets in regenerating *CIP2A*^{HOZ} intestine (Figure 6I).

Together, these results provide in vivo validation that CIP2A selectively supports the expression of serine 62-phosphorylated MYC.

Confirmation of the Importance of MYC Serine 62 Phosphorylation for Proliferation Induction In Vivo

To validate our main conclusion that expression of pS62MYC is critical for proliferation induction in vivo, we again used the MYC serine 62 phosphorylation mutants in an in vivo setting. We hypothesized that T58A might more potently rescue the effects of endogenous MYC loss in the intestinal regeneration model than WT MYC and S62A MYC. We have shown recently that WT c-*myc* (*Rosa*$^{Myc/+}$) transgene expression at a subphysiological level is unable to drive a regenerative response in the absence of endogenous, Wnt-induced c-*myc* (Ashton et al., 2010).

To this end, we crossed *AhCre Myc*$^{fl/fl}$ mice with mice carrying a *Lox-stop-Lox c-myc*, *Lox-stop-Lox c-myc*^{T58A}, and *Lox-stop-Lox c-myc*^{S62A} allele to generate *Myc*$^{fl/fl}$ *Rosa*$^{Myc/+}$, *Myc*$^{fl/fl}$ *Rosa*$^{MycT58A/+}$, and *Myc*$^{fl/fl}$ *Rosa*$^{MycS62A/+}$ mice, respectively (Figure S6A). This cross permits B-napthoflavone-induced expression of either the WT, T58A, or S62A allele of MYC at subphysiological levels in the absence of endogenous, Wnt-induced c-*myc*. Importantly, upon recombination, the transgenes were transcriptionally expressed at the same level (Figure S6B), whereas both T58AMYC and S62AMYC showed significantly higher protein expression in regenerating intestine than WT MYC (Figure 7A). Increased expression of the T58A mutant is presumably due to its higher protein stability, whereas higher protein expression of S62MYC than WT MYC upon tissue

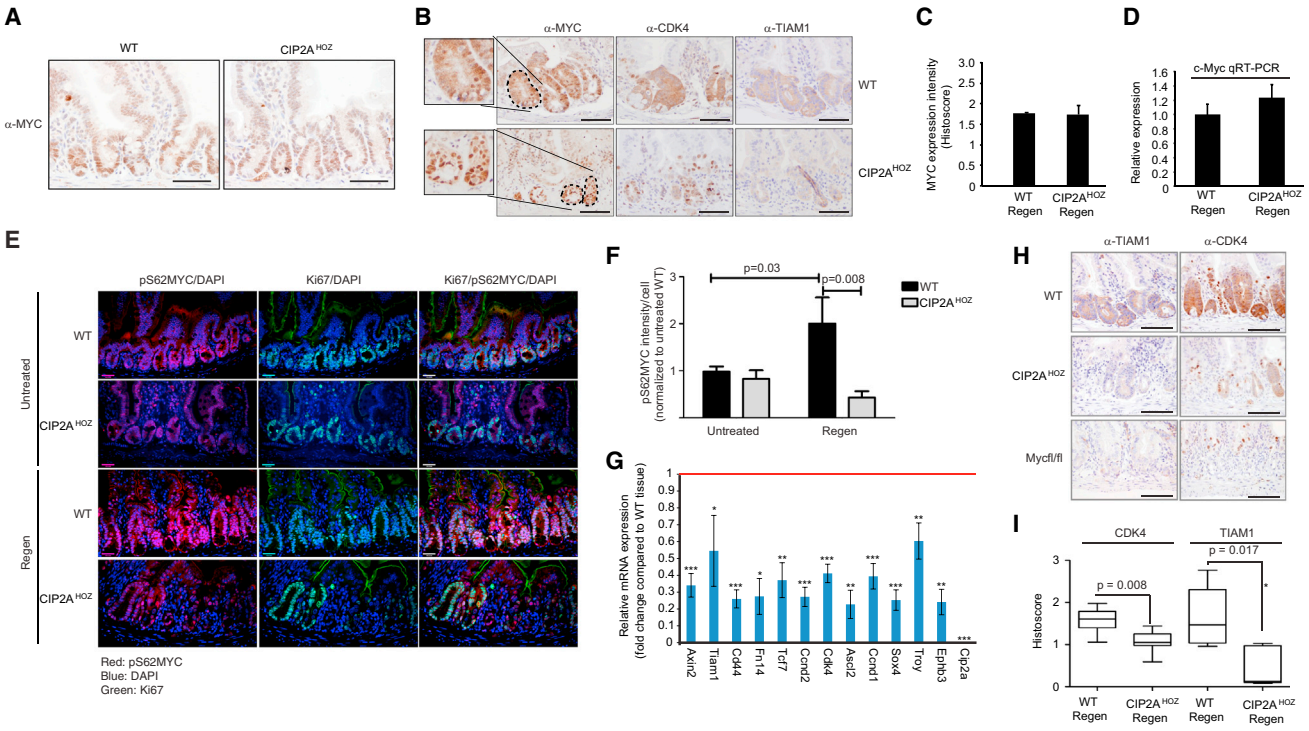

Figure 6. CIP2A Is Critical for the Expression of Serine 62-Phosphorylated MYC and for MYC-Driven Transcriptional Activity during In Vivo Proliferation Induction

(A) Immunohistochemical staining of MYC from untreated WT and *CIP2A*^{HOZ} intestines. Scale bars, 50 μm.

(B) Immunohistochemical staining of MYC, CDK4, and TIAM1 in regenerating crypts from WT and *CIP2A*^{HOZ} intestines. The dashed line outlines the crypt area used for histoscoring. The insets show magnified images of MYC staining intensity in selected crypts. Scale bars, 50 μm.

(C) Histoscoring of the intensity of MYC immunopositivity in regenerating crypts from WT and *CIP2A*^{HOZ} intestines (p = not significant, Mann-Whitney test, n = 3 versus 3).

(D) qRT-PCR analysis of MYC in WT regenerating and *CIP2A*^{HOZ} regenerating small intestines (p = not significant, Student's t test, n = 6). Error bars represent the mean ± SD.

(E) Immunofluorescent staining for pS62MYC in WT, *CIP2A*^{HOZ}, WT regenerating, and *CIP2A*^{HOZ} regenerating small intestines. Ki67 was co-stained to assess the induction of proliferation. Scale bars, 25 μm. Magnification, ×20.

(F) Quantitation of pS62MYC intensity per cell from (E). Error bars represent the mean ± SD.

(G) qRT-PCR analysis for MYC target gene expression in WT regenerating and *CIP2A*^{HOZ} regenerating small intestines (*p < 0.05, **p < 0.01, ***p < 0.001; Student's t test, n = 3). The red line represents mRNA expression levels of MYC target genes normalized to 1 in wild-type tissue. Error bars represent mean ± SD.

(H) Immunohistochemical staining of TIAM1 and CDK4 in regenerating crypts from WT, *CIP2A*^{HOZ}, and *Myc*$^{fl/fl}$ intestines. Scale bars, 50 μm.

(I) Histoscoring of CDK4 and TIAM1 immunopositivity in regenerating crypts from WT and *CIP2A*^{HOZ} intestines (Mann-Whitney test, n = 6 versus 7). The data are derived from a tissue section adjacent to that analyzed for the MYC histoscore in (B). The asterisk indicates an outlier value removed from the analysis.

regeneration may be due to a compensation mechanism, as discussed below. However, despite the similar protein expression levels of T58AMYC and S62AMYC, as assessed by a total MYC antibody, the MYCT58A mutant did show a significantly increased level of serine 62 phosphorylation in regenerating intestine tissue compared with either S62A or WT MYC (Figures 7B and 7C). This finding is consistent with data published previously (Lutterbach and Hann, 1994; Sears et al., 2000) and allows comparison of these models to assess whether the form of MYC that drives the highest regeneration potential in vivo is the serine 62-phosphorylated MYC. Irradiation of WT mice again resulted in a robust regenerative response 72 hr later, as evidenced by large crypts that stained positively for Ki67 (Figure 7D; Figure S6C). However, the conditional deletion of *c-myc* by intraperitoneal (i.p.) injection of B-napthoflavone (*Myc*$^{fl/fl}$) suppressed regeneration (Figure 7D; Figure S6C). As shown before (Ashton et al., 2010), the B-naphtoflavone injection-elicited expression of WT c-*myc* (*Rosa*$^{Myc/+}$) at a subphysiological level was unable to drive a regenerative response (Figure 7D; Figure S6C). However, consistent with all other data indicating that serine 62 phosphorylation defines MYC's proliferative potential, T58AMYC was significantly more competent than the WT of S62AMYC to compensate for the loss of endogenous c-*myc,* both in the regeneration response as well as in driving cell proliferation in response to irradiation (Figures 7D and 7E; Figure S6C). Importantly, we did not observe any gross histological differences or proliferative effects following expression of the T58AMYC transgene in untreated wild-type mice, indicating that the increased regeneration by T58AMYC was not due to a more proliferative environment (Figure S6D). Furthermore, in full support of our in vitro results showing that serine 62 phosphorylation is a determining factor for whether MYC interacts with both CIP2A

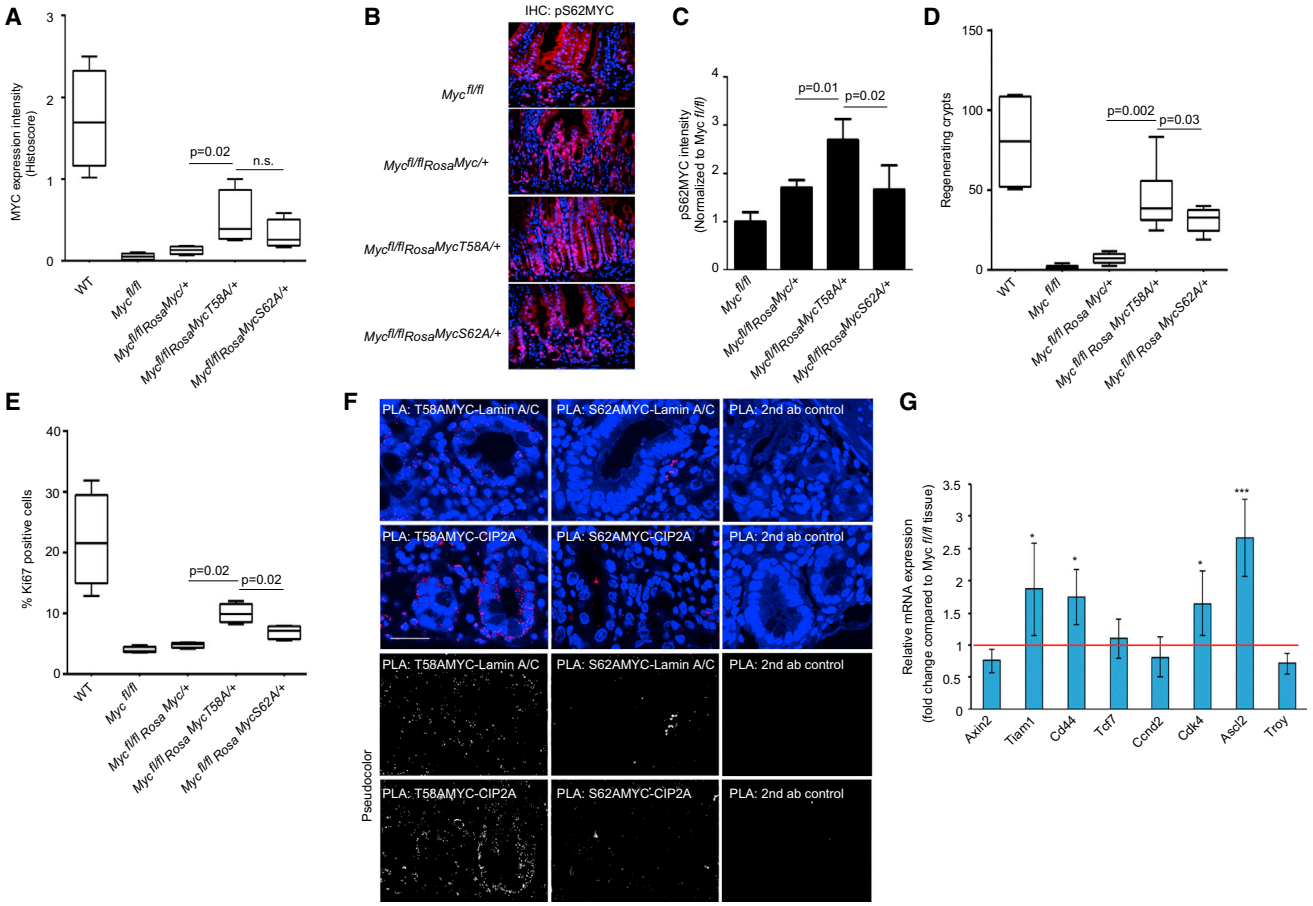

Figure 7. Analysis of MYC Knockin Mutants Support the Importance of MYC Serine 62 Phosphorylation and Lamin A/C Association for Proliferation Induction In Vivo

(A) Quantitation of MYC immunostaining intensity in regenerating small intestine in mice with the indicated genotypes (Mann-Whitney test, n = 4 versus 4).

(B) Immunofluorescent staining for pS62MYC in regenerating small intestine in mice with the indicated genotypes. Magnification, ×20.

(C) Quantitation of pS62MYC intensity from (B) (Mann-Whitney test, n = 4 versus 4).

(D) Scoring of regenerating crypts in mice with the indicated genotypes 72 hr post-irradiation.

(E) Scoring of the percentage of Ki67-positive cells per crypt in mice with the indicated genotypes 72 hr post-irradiation.

(F) PLA analysis of the MYC-Lamin A/C and MYC-CIP2A association in intestinal crypts in mice with the indicated genotypes 72 hr post-irradiation. The specificity of PLA is shown by the lack of PLA signals in the secondary antibody-only control panel. Scale bar, 25 μm.

(G) qRT-PCR analysis for CIP2A-regulated MYC target gene expression in *Myc*$^{fl/fl}$ and *Myc*$^{fl/fl}$ *Rosa*$^{MycT58A/+}$ small intestine (*p < 0.05, **p < 0.01, ***p < 0.001; Student's t test; n = 3). The red line represents mRNA expression levels of CIP2A-regulated MYC target genes normalized to 1 in *Myc*$^{fl/fl}$ small intestine. Error bars represent the mean ± SD.

(Junttila et al., 2007) and Lamin A/C (Figures 2A–2C), the PLA analysis on regenerating intestinal tissues demonstrated an almost absolute lack of LAS localization of MYCS62A, whereas MYCT58A robustly interacted with both CIP2A and Lamin A/C in vivo (Figure 7F). Finally, we confirmed that expression of MYCT58A also rescued the expression of a number of CIP2A-regulated MYC target genes that were downregulated in *Myc*$^{fl/fl}$ intestine (Figure 7G). Importantly, among those that were rescued was Tiam1, which was used as a model gene to demonstrate CIP2A's role in MYC promoter recruitment (Figure S5).

Together, these results strongly support our main conclusions that the form of MYC protein that drives in vivo proliferation and DNA damage-induced regeneration is pS62MYC and that the association of pS62MYC with both the LAS and CIP2A is intimately linked to MYC-mediated proliferation induction and gene expression in vivo.

DISCUSSION

The development of targeted therapies requires a thorough understanding of the molecular mechanisms regulating the target activity as well as the validation of the importance of this mechanism in a faithful in vivo model. Based on extensive research during the past three decades, it has become evident that targeting of MYC would be highly desirable for hyperproliferative diseases (Meyer and Penn, 2008; Soucek et al., 2008). Surprisingly, though, until now it has not been demonstrated which endogenous post-translational mechanism defines MYC activity in vivo.

In this work, we demonstrate, by using both CIP2A and MYC mouse models, that CIP2A-mediated support of MYC serine 62 phosphorylation is critically linked to MYC's capacity to re-initiate proliferation and support intestinal regeneration in response to DNA damage. Importantly, our data indicate that neither CIP2A nor MYC serine 62 phosphorylation impact basal proliferation or differentiation of intestinal crypt cells. Therefore, MYC serine 62 phosphorylation appears to be selectively required to support MYC-mediated high-level proliferation. In addition to their biological importance, these results indicate that selective targeting of mechanisms that support serine 62 phosphorylation MYC might constitute a therapy strategy for hyperproliferative diseases. Specifically, the results indicate that targeting CIP2A could offer a possibility to interfere with MYC-mediated proliferation without detrimental consequences on normal physiology. However, we cannot currently exclude that, in addition to MYC, inhibition of other CIP2A-regulated proteins (Khanna et al., 2013; Puustinen et al., 2014) could also partly contribute to the in vivo effects of CIP2A inhibition in intestinal regeneration. On the other hand, the results imply that pharmaceutical inhibition of CIP2A might affect the regeneration of normal tissues when combined with DNA-damaging anticancer drugs. Therefore, targeting of CIP2A should be combined, for example, with localized radiotherapy specifically targeting the tumor tissue. In support of the importance of CIP2A in mediating radioresistance in human cancers, we recently published a study showing that high expression of tumor CIP2A and stem cell factor Oct4 predicts poor patient survival in cancer patients treated with radiotherapy (Ventela et al., 2015).

Even though serine 62 phosphorylation regulates MYC stability in cultured cells (Hann, 2006; Sears et al., 2000), our data show that, upon irradiation-induced proliferation in vivo, loss of endogenous MYC serine 62 phosphorylation by CIP2A inhibition does not abrogate total MYC expression (Figures 6B and 6C). Interestingly, the S62AMYC mutant also did not show a significant difference in protein expression compared with T58AMYC. We speculate that either there is a fundamental difference in the role of serine 62 phosphorylation or MYC in its stability regulation between the in vitro and in vivo context or that, upon loss of serine 62 phosphorylation in vivo, intestinal cells under DNA damage-induced stress compensate for the situation by increasing the expression of MYC that is not phosphorylated on serine 62 by a still unknown mechanism. We also cannot exclude that the non-significant decreased median expression of S62AMYC may, in part, contribute to the proliferation defect caused by loss of serine 62 phosphorylation. We even noted some focus-positive staining with pS62MYC antibody in the nucleus of $MYC^{fl/fl}$ mice, and this can be due to compensatory expression of NMYC because the sequences surrounding serine 62 are nearly 100% conserved between MYC and NMYC.

Importantly, the cell culture experiments revealed a plausible explanation for the selectivity of CIP2A toward pS62MYC. We show that serine 62 phosphorylation promotes MYC recruitment to the LAS and that only pS62MYC associated with the LAS is sensitive to regulation by CIP2A, whereas MYC in the soluble nuclear fraction was resistant to CIP2A depletion. Importantly, the preferential association of T58AMYC, exhibiting increased serine 62 phosphorylation, with the LAS and CIP2A was validated in vivo (Figure 7F). Most importantly, the functional outcomes of both the $CIP2A^{HOZ}$ and S62AMYC models perfectly support the overall conclusions of this work that, when MYC is phosphorylated on serine 62, it interacts with both LAS and CIP2A and that this biochemical form of MYC drives in vivo proliferation and regeneration.

Consistent with an emerging picture of nuclear lamin-associated domains as critical structures for gene regulation and chromatin remodeling (Kind et al., 2013; Shimi et al., 2010; Zullo et al., 2012), our data indicate that CIP2A-MYC interaction at the LAS is essential for maintaining transcription-competent MYC that subsequently binds to its target promoters to promote the expression of proliferation-inducing genes. Importantly, recent studies have also indicated that serine 62 phosphorylation of MYC may affect target promoter selection (Benassi et al., 2006; Farrell et al., 2013), which is another interesting aspect to study in the future by using a CIP2A-deficient mouse model. Also, the association of CIP2A with nuclear pores (data not shown; Thakar et al., 2013) is consistent with the recent indication that multiprotein platforms at nuclear pores are key regulators of the DNA damage response (Arib and Akhtar, 2011; Bukata et al., 2013). Of historical note, association of MYC with the nuclear envelope has been demonstrated previously (Eisenman et al., 1985; Winqvist et al., 1984), and MYC stability has been linked to its subnuclear partitioning (Tworkowski et al., 2002), but the physiological relevance of these findings has so far been obscure.

In summary, these results demonstrate that MYC serine 62 phosphorylation is a non-essential mechanism that supports MYC's proliferative activity in vivo. Because CIP2A supports pS62MYC expression and other oncogenic driver phosphorylation events (Khanna et al., 2013) but is non-essential in normal physiology, the development of chemical inhibitors of CIP2A is a prospective approach for the inhibition of proliferation in vivo without therapy-limiting side effects. We also envision that our results will provoke future studies to identify other therapeutic strategies to inhibit MYC serine 62 phosphorylation. Moreover, our demonstration that transcription factor function and accumulation are regulated at the LAS suggests the potential for targeting these structures for future therapies. Finally, our data demonstrate CIP2A as a signaling protein that is indispensable for the efficient recovery and regeneration of intestinal tissue in response to DNA damage, implying an important role for CIP2A in organismal DNA damage response.

EXPERIMENTAL PROCEDURES

Mouse Experiments

All experiments were performed under UK Home Office guidelines. All mice used were of a mixed background (50% C57BlJ, 50% S129). The alleles used for this study were as follows: $c\text{-}Myc^{fl}$ (de Alboran et al., 2001), *AhCre* (Ireland et al., 2004), $Rosa^{Myc}$ (Wang et al., 2011), $Rosa^{MycT58}$ (Wang et al., 2011), and $CIP2A^{HOZ}$ (Ventelä et al., 2012). To determine the role of Myc protein stability during intestinal regeneration, *AhCre* $c\text{-}Myc^{fl/fl}$ mice were crossed to $Rosa^{Myc}$, $Rosa^{MycT58A}$, or $Rosa^{MycS62A}$ mice. Control, *AhCre* $c\text{-}Myc^{fl/fl}$, *AhCre* $c\text{-}Myc^{fl/fl}$ $Rosa^{Myc/+}$, *AhCre* $c\text{-}Myc^{fl/fl}$ $Rosa^{MycT58A/+}$, or *AhCre* $c\text{-}Myc^{fl/fl}$ $Rosa^{MycS62A/+}$ mice were given three i.p. injections of 80 mg/kg β-napthoflavone in a single day, which yields nearly constitutive recombination in the murine small intestine. Intestinal regeneration experiments have been described previously (Myant et al., 2013), and the protocol is included in the Supplemental Experimental Procedures.

Immunohistochemistry

Standard immunohistochemistry techniques were used throughout this study. The primary antibodies used for immunohistochemistry were as follows: Ki67 (Vector Laboratories, catalog no. VP-K452), c-Myc (Santa Cruz Biotechnology, catalog no. sc-764), BrdUrd (BD Biosciences), CDK4 (Santa Cruz, catalog no. sc-260), Tiam1 (Santa Cruz, sc-872), CIP2A (Junttila et al., 2007; Laine et al., 2013; Soo Hoo et al., 2002; Ventelä et al., 2012), and pS62MYC(Junttila et al., 2007; Wang et al., 2011; Yeh et al., 2004). Immunohistochemistry was performed on formalin-fixed intestinal sections. For each antibody, staining was performed on at least three mice of each genotype. For histoscoring, the average staining intensity in 50 consecutive crypts was scored from at least six mice. For MYC serine 62 phosphorylation, the fluorescent signals for pS62MYC intensity and 4′,6-diamidino-2-phenylindole (DAPI) intensity were calculated from four slides, each representing a different treatment/phenotype. From these, ten pictures per slide were taken, and from each picture, nucleus staining was quantified by drawing a circle around 20 nuclei using the OpenLab 5.5 software, and the signal intensity was measured from 50 nuclei/crypt from each picture using ImageJ. MYC phosphorylation status is expressed as the pS62MYC/DAPI ratio using the average intensity from all measurements per treatment/genotype. Error bars represent the averaged intensity calculated in four mice. Similar results were obtained from two independent series of experiments performed one year apart. Representative images are shown for each staining. The scale bars in all figures represent 50 μm.

Proximity Ligation Assay and Immunofluorescence Staining

The PLA assay was performed according to the manufacturer's protocol (Olink Bioscience). Briefly, cells plated on coverslips were grown to 70% confluence, fixed with 3:1 acetone methanol at −20°C for 5–7 min, blocked with blocking solution, and incubated in a pre-heated humidity chamber for 30 min at 37°C, followed by incubating the primary antibodies (in blocking solution) anti-CIP2A (Soo Hoo et al., 2002), anti-CIP2A (catalog no. sc-80659, Santa Cruz), anti-MYC (catalog no. 9E10, Sigma), anti-Lamin A/C (goat, catalog no. sc-6215, Santa Cruz), anti-LAP2 (catalog no. 611000, BD Transduction Laboratories), anti-Lamin A/C (636, mouse, catalog no. sc-7292, Santa Cruz), anti-Lamin A/C (H-110, rabbit, catalog no. sc-20681, Santa Cruz), and anti-c-Myc (phosphoserine 62, mouse, catalog no. ab78318, Abcam) overnight at 4°C. Subsequently, cells were washed with buffer A, and the PLA probe was incubated in a pre-heated humidity chamber for 1 hr at 37°C, followed by ligase reaction in a pre-heated humidity chamber for 1 hr at 37°C. Next, amplification polymerase solution for PLA and the secondary antibody Alexa Fluor 488 (Invitrogen) for Lamin A/C (goat, catalog no. sc-6215, Santa Cruz), used for CIP2A-MYC and CIP2A-pS62MYC PLA, were added, followed by incubating the cells in a pre-heated humidity chamber for 100 min at 37°C.

For tissue samples, formalin-fixed slides were dewaxed in xylene and rehydrated in decreasing concentrations of alcohol, followed by washing two times in tap water. The slides were then incubated in antigen retrieval buffer (Lab Vision citrate buffer, Thermo Scientific) for 30 min at 99°C, followed by cooling down to room temperature and rinsing the slides in distilled water (dH_2O). Next, the slides were blocked for 15 min in 1.5% H_2O_2 solution in PBS, followed by rising in dH_2O and rinsing once in Tris-buffered saline with Tween 20 (TBST) buffer. Finally, the PLA assay was performed following the PLA protocol for cell staining from blocking slides by blocking solution. Immunofluorescence for CIP2A, MYC (catalog no. sc-764, Santa Cruz), pS62MYC (catalog no. ab51156, Abcam), and Lamin A/C (catalog no. sc-7292, Santa Cruz) was performed as described previously (Junttila et al., 2007). All fluorescent stainings were analyzed using a confocal microscope (LSM780, Carl Zeiss).

SUPPLEMENTAL INFORMATION

Supplemental Information includes Supplemental Experimental Procedures and six figures and can be found with this article online at http://dx.doi.org/10.1016/j.celrep.2015.07.003.

AUTHOR CONTRIBUTIONS

K.M. contributed to Figures 4A, 4D, 4E, 5, 6, 7, and S4. X.Q. contributed to Figures 1A, 1C–1G, 1I, 1J, 2C, 2F, 2G, 4B–4F, 7F, S1A, and S2. T.H. contributed to Figures 1B, 1H, 2A, 2D, 3E, S1B, and S5. C.C. contributed to the development and characterization of the $CIP2A^{HOZ}$ mouse strain. A.L. contributed to Figures 3A–3D, 3F, 3G, 3I, and S3. M.J. contributed to Figures 6E, 6F, 7B, and 7C. J.I.P contributed to Figures 3H and 3I. J.C, E.L.O., and P.C. contributed to the tissue analysis of transgenic mouse models. T.L. contributed to Figures 3A, 3F, and 3G. J.O. contributed to supervision and data analysis. J.K contributed to experimental planning, data analysis, and manuscript writing. R.C.S provided the MYC phosphorylation mutant mice and contributed to experimental planning and data analysis. O.J.S. contributed to supervision, concept and experiment planning, data analysis, and manuscript writing. J.W. contributed to supervision, concept and experiment planning, data analysis, and manuscript writing.

ACKNOWLEDGMENTS

We thank Prof. Martin Eilers, Prof. Johanna Ivaska, Dr. Pekka Taimen, and Dr. Daniel Abankwa for critical reading of the manuscript and Prof. Bruno Amati for his valuable advice regarding ChIP analysis. Taina Kalevo-Mattila is thanked for technical help and Jouko Sandström and Markku Saari at the Turku Centre for Biotechnology Cell Imaging Core facility for help with imaging. This study was supported by funding from the Association of International Cancer Research (grants 08-0614 and 10-0643), the Academy of Finland (grants 122546, 137687, and 267817), Finnish Cancer Organisations, the Foundation of Finnish Cancer Institute, the Sigrid Juselius Foundation, the NIH (grants R01 CA129040 and R01 CA100855), The European Research Council (Coloncan), European Commission FP7-Health (grant 278568), and Cancer Research UK (grant A12481).

Received: December 27, 2013
Revised: April 24, 2015
Accepted: July 1, 2015
Published: July 30, 2015

REFERENCES

Arib, G., and Akhtar, A. (2011). Multiple facets of nuclear periphery in gene expression control. Curr. Opin. Cell Biol. *23*, 346–353.

Ashton, G.H., Morton, J.P., Myant, K., Phesse, T.J., Ridgway, R.A., Marsh, V., Wilkins, J.A., Athineos, D., Muncan, V., Kemp, R., et al. (2010). Focal adhesion kinase is required for intestinal regeneration and tumorigenesis downstream of Wnt/c-Myc signaling. Dev. Cell *19*, 259–269.

Athineos, D., and Sansom, O.J. (2010). Myc heterozygosity attenuates the phenotypes of APC deficiency in the small intestine. Oncogene *29*, 2585–2590.

Benassi, B., Fanciulli, M., Fiorentino, F., Porrello, A., Chiorino, G., Loda, M., Zupi, G., and Biroccio, A. (2006). c-Myc phosphorylation is required for cellular response to oxidative stress. Mol. Cell *21*, 509–519.

Bukata, L., Parker, S.L., and D'Angelo, M.A. (2013). Nuclear pore complexes in the maintenance of genome integrity. Curr. Opin. Cell Biol. *25*, 378–386.

Capelson, M., Doucet, C., and Hetzer, M.W. (2010). Nuclear pore complexes: guardians of the nuclear genome. Cold Spring Harb. Symp. Quant. Biol. *75*, 585–597.

de Alboran, I.M., O'Hagan, R.C., Gärtner, F., Malynn, B., Davidson, L., Rickert, R., Rajewsky, K., DePinho, R.A., and Alt, F.W. (2001). Analysis of C-MYC function in normal cells via conditional gene-targeted mutation. Immunity *14*, 45–55.

Dechat, T., Adam, S.A., Taimen, P., Shimi, T., and Goldman, R.D. (2010). Nuclear lamins. Cold Spring Harb. Perspect. Biol. *2*, a000547.

Dubois, N.C., Adolphe, C., Ehninger, A., Wang, R.A., Robertson, E.J., and Trumpp, A. (2008). Placental rescue reveals a sole requirement for c-Myc in embryonic erythroblast survival and hematopoietic stem cell function. Development *135*, 2455–2465.

Eisenman, R.N., Tachibana, C.Y., Abrams, H.D., and Hann, S.R. (1985). V-myc- and c-myc-encoded proteins are associated with the nuclear matrix. Mol. Cell. Biol. *5*, 114–126.

Farrell, A.S., Pelz, C., Wang, X., Daniel, C.J., Wang, Z., Su, Y., Janghorban, M., Zhang, X., Morgan, C., Impey, S., and Sears, R.C. (2013). Pin1 regulates the dynamics of c-Myc DNA binding to facilitate target gene regulation and oncogenesis. Mol. Cell. Biol. *33*, 2930–2949.

Finch, A.J., Soucek, L., Junttila, M.R., Swigart, L.B., and Evan, G.I. (2009). Acute overexpression of Myc in intestinal epithelium recapitulates some but not all the changes elicited by Wnt/beta-catenin pathway activation. Mol. Cell. Biol. *29*, 5306–5315.

Hann, S.R. (2006). Role of post-translational modifications in regulating c-Myc proteolysis, transcriptional activity and biological function. Semin. Cancer Biol. *16*, 288–302.

Ireland, H., Kemp, R., Houghton, C., Howard, L., Clarke, A.R., Sansom, O.J., and Winton, D.J. (2004). Inducible Cre-mediated control of gene expression in the murine gastrointestinal tract: effect of loss of beta-catenin. Gastroenterology *126*, 1236–1246.

Janssens, V., and Goris, J. (2001). Protein phosphatase 2A: a highly regulated family of serine/threonine phosphatases implicated in cell growth and signalling. Biochem. J. *353*, 417–439.

Junttila, M.R., Puustinen, P., Niemelä, M., Ahola, R., Arnold, H., Böttzauw, T., Ala-aho, R., Nielsen, C., Ivaska, J., Taya, Y., et al. (2007). CIP2A inhibits PP2A in human malignancies. Cell *130*, 51–62.

Khanna, A., Pimanda, J.E., and Westermarck, J. (2013). Cancerous inhibitor of protein phosphatase 2A, an emerging human oncoprotein and a potential cancer therapy target. Cancer Res. *73*, 6548–6553.

Kim, J.S., Kim, E.J., Oh, J.S., Park, I.C., and Hwang, S.G. (2013). CIP2A modulates cell cycle progression in human cancer cells by regulating the stability and activity of PLK1. Cancer Res. *73*, 6667–6678.

Kind, J., Pagie, L., Ortabozkoyun, H., Boyle, S., de Vries, S.S., Janssen, H., Amendola, M., Nolen, L.D., Bickmore, W.A., and van Steensel, B. (2013). Single-cell dynamics of genome-nuclear lamina interactions. Cell *153*, 178–192.

Laine, A., Sihto, H., Come, C., Rosenfeldt, M.T., Zwolinska, A., Niemelä, M., Khanna, A., Chan, E.K., Kähäri, V.M., Kellokumpu-Lehtinen, P.L., et al. (2013). Senescence sensitivity of breast cancer cells is defined by positive feedback loop between CIP2A and E2F1. Cancer Discov. *3*, 182–197.

Lüscher, B., and Vervoorts, J. (2012). Regulation of gene transcription by the oncoprotein MYC. Gene *494*, 145–160.

Lutterbach, B., and Hann, S.R. (1994). Hierarchical phosphorylation at N-terminal transformation-sensitive sites in c-Myc protein is regulated by mitogens and in mitosis. Mol. Cell. Biol. *14*, 5510–5522.

Mateyak, M.K., Obaya, A.J., Adachi, S., and Sedivy, J.M. (1997). Phenotypes of c-Myc-deficient rat fibroblasts isolated by targeted homologous recombination. Cell Growth Differ. *8*, 1039–1048.

Metcalfe, C., Kljavin, N.M., Ybarra, R., and de Sauvage, F.J. (2014). Lgr5+ stem cells are indispensable for radiation-induced intestinal regeneration. Cell Stem Cell *14*, 149–159.

Meyer, N., and Penn, L.Z. (2008). Reflecting on 25 years with MYC. Nat. Rev. Cancer *8*, 976–990.

Muncan, V., Sansom, O.J., Tertoolen, L., Phesse, T.J., Begthel, H., Sancho, E., Cole, A.M., Gregorieff, A., de Alboran, I.M., Clevers, H., and Clarke, A.R. (2006). Rapid loss of intestinal crypts upon conditional deletion of the Wnt/Tcf-4 target gene c-Myc. Mol. Cell. Biol. *26*, 8418–8426.

Myant, K.B., Cammareri, P., McGhee, E.J., Ridgway, R.A., Huels, D.J., Cordero, J.B., Schwitalla, S., Kalna, G., Ogg, E.L., Athineos, D., et al. (2013). ROS production and NF-κB activation triggered by RAC1 facilitate WNT-driven intestinal stem cell proliferation and colorectal cancer initiation. Cell Stem Cell *12*, 761–773.

Niemelä, M., Kauko, O., Sihto, H., Mpindi, J.P., Nicorici, D., Pernilä, P., Kallioniemi, O.P., Joensuu, H., Hautaniemi, S., and Westermarck, J. (2012). CIP2A signature reveals the MYC dependency of CIP2A-regulated phenotypes and its clinical association with breast cancer subtypes. Oncogene *31*, 4266–4278.

Nieminen, A.I., Partanen, J.I., Hau, A., and Klefstrom, J. (2007). c-Myc primed mitochondria determine cellular sensitivity to TRAIL-induced apoptosis. EMBO J. *26*, 1055–1067.

Perna, D., Fagà, G., Verrecchia, A., Gorski, M.M., Barozzi, I., Narang, V., Khng, J., Lim, K.C., Sung, W.K., Sanges, R., et al. (2012). Genome-wide mapping of Myc binding and gene regulation in serum-stimulated fibroblasts. Oncogene *31*, 1695–1709.

Puustinen, P., Rytter, A., Mortensen, M., Kohonen, P., Moreira, J.M., and Jäättelä, M. (2014). CIP2A oncoprotein controls cell growth and autophagy through mTORC1 activation. J. Cell Biol. *204*, 713–727.

Sansom, O.J., Meniel, V.S., Muncan, V., Phesse, T.J., Wilkins, J.A., Reed, K.R., Vass, J.K., Athineos, D., Clevers, H., and Clarke, A.R. (2007). Myc deletion rescues Apc deficiency in the small intestine. Nature *446*, 676–679.

Sears, R., Leone, G., DeGregori, J., and Nevins, J.R. (1999). Ras enhances Myc protein stability. Mol. Cell *3*, 169–179.

Sears, R., Nuckolls, F., Haura, E., Taya, Y., Tamai, K., and Nevins, J.R. (2000). Multiple Ras-dependent phosphorylation pathways regulate Myc protein stability. Genes Dev. *14*, 2501–2514.

Shimi, T., Butin-Israeli, V., Adam, S.A., and Goldman, R.D. (2010). Nuclear lamins in cell regulation and disease. Cold Spring Harb. Symp. Quant. Biol. *75*, 525–531.

Soo Hoo, L., Zhang, J.Y., and Chan, E.K. (2002). Cloning and characterization of a novel 90 kDa 'companion' auto-antigen of p62 overexpressed in cancer. Oncogene *21*, 5006–5015.

Soucek, L., Whitfield, J., Martins, C.P., Finch, A.J., Murphy, D.J., Sodir, N.M., Karnezis, A.N., Swigart, L.B., Nasi, S., and Evan, G.I. (2008). Modelling Myc inhibition as a cancer therapy. Nature *455*, 679–683.

Thakar, K., Karaca, S., Port, S.A., Urlaub, H., and Kehlenbach, R.H. (2013). Identification of CRM1-dependent nuclear export cargos using quantitative mass spectrometry. Mol. Cell. Proteomics *12*, 664–678.

Thomas, L.R., and Tansey, W.P. (2011). Proteolytic control of the oncoprotein transcription factor Myc. Adv. Cancer Res. *110*, 77–106.

Trumpp, A., Refaeli, Y., Oskarsson, T., Gasser, S., Murphy, M., Martin, G.R., and Bishop, J.M. (2001). c-Myc regulates mammalian body size by controlling cell number but not cell size. Nature *414*, 768–773.

Tworkowski, K.A., Salghetti, S.E., and Tansey, W.P. (2002). Stable and unstable pools of Myc protein exist in human cells. Oncogene *21*, 8515–8520.

van der Flier, L.G., Haegebarth, A., Stange, D.E., van de Wetering, M., and Clevers, H. (2009). OLFM4 is a robust marker for stem cells in human intestine and marks a subset of colorectal cancer cells. Gastroenterology *137*, 15–17.

Ventelä, S., Côme, C., Mäkelä, J.A., Hobbs, R.M., Mannermaa, L., Kallajoki, M., Chan, E.K., Pandolfi, P.P., Toppari, J., and Westermarck, J. (2012). CIP2A promotes proliferation of spermatogonial progenitor cells and spermatogenesis in mice. PLoS ONE *7*, e33209.

Ventela, S., Sittig, E., Mannermaa, L., Makela, J.A., Kulmala, J., Loyttyniemi, E., Strauss, L., Carpen, O., Toppari, J., Grenman, R., et al. (2015). CIP2A is an Oct4 target gene involved in head and neck squamous cell cancer oncogenicity and radioresistance. Oncotarget *6*, 144–158.

Wang, X., Cunningham, M., Zhang, X., Tokarz, S., Laraway, B., Troxell, M., and Sears, R.C. (2011). Phosphorylation regulates c-Myc's oncogenic activity in the mammary gland. Cancer Res. *71*, 925–936.

Winqvist, R., Saksela, K., and Alitalo, K. (1984). The myc proteins are not associated with chromatin in mitotic cells. EMBO J. *3*, 2947–2950.

Yeh, E., Cunningham, M., Arnold, H., Chasse, D., Monteith, T., Ivaldi, G., Hahn, W.C., Stukenberg, P.T., Shenolikar, S., Uchida, T., et al. (2004). A signalling pathway controlling c-Myc degradation that impacts oncogenic transformation of human cells. Nat. Cell Biol. *6*, 308–318.

Zullo, J.M., Demarco, I.A., Piqué-Regi, R., Gaffney, D.J., Epstein, C.B., Spooner, C.J., Luperchio, T.R., Bernstein, B.E., Pritchard, J.K., Reddy, K.L., and Singh, H. (2012). DNA sequence-dependent compartmentalization and silencing of chromatin at the nuclear lamina. Cell *149*, 1474–1487.